Refined Crystal Structure of Adenylosuccinate Synthetase from Escherichia coli Complexed with Hydantocidin 5‘-Phosphate, GDP, HPO 4 2- , Mg 2+ , and Hadacidin † , ‡

ARTICLE *in* BIOCHEMISTRY · JANUARY 1997

Impact Factor: 3.02 · DOI: 10.1021/bi961758r · Source: PubMed

7 AUTHORS, INCLUDING:

Daniel Siehl
DuPont Pioneer, Hayward, CA
30 PUBLICATIONS **1,024** CITATIONS

SEE PROFILE

Refined Crystal Structure of Adenylosuccinate Synthetase from *Escherichia coli* Complexed with Hydantocidin 5′-Phosphate, GDP, HPO_4^{2-}, Mg^{2+}, and Hadacidin[†,‡]

Bradley W. Poland,[§] Shy-Fuh Lee,[||] Mani V. Subramanian,[||] Daniel L. Siehl,[||] Richard J. Anderson,[||] Herbert J. Fromm,[§] and Richard B. Honzatko*[,§]

Department of Biochemistry and Biophysics, 1210 Molecular Biology Building, Iowa State University, Ames, Iowa 50011, and Sandoz Agro, Inc., 975 California Avenue, Palo Alto, California 94304-1104

Received July 17, 1996; Revised Manuscript Received October 15, 1996[⊗]

ABSTRACT: A crystal structure of adenylosuccinate synthetase from *Escherichia coli*, complexed with 5′-phosphate, GDP, HPO_4^{2-}, Mg^{2+}, and hadacidin at 100 K, has been refined to an R_{factor} of 0.195 against data to 2.6 Å resolution. Bond lengths and angles deviate from expected values by 0.012 Å and 1.86°, respectively. Lys 16 and backbone amides 15−17 and 42 interact with the phosphates of GDP, while Ser 414, Asp 333, and backbone amides 331 and 416 interact with the base. Mg^{2+} is octahedrally coordinated. Oxygen atoms from GDP, phosphate, and hadacidin define the equatorial plane of coordination of the Mg^{2+}, while backbone carbonyl 40 and the side chain of Asp 13 are the apical ligands. HPO_4^{2-} hydrogen bonds with Lys 16, His 41, backbone amides 13, 40, and 224, and the base moiety of the hydantocidin inhibitor. The carboxylate of hadacidin interacts with Arg 303 and Thr 301; its *N*-formyl group coordinates to Mg^{2+}, and its hydroxyl group hydrogen bonds with Asp 13. The 5′-phosphate of the hydantocidin inhibitor interacts with Asn 38, Thr 129, and Thr 239 but is approximately 3.5 Å from Arg 143 (related by molecular 2-fold symmetry). The base moiety of hydantocidin 5′-phosphate hydrogen bonds to Gln 224 and participates in a hydrogen-bonded network that includes the phosphate molecule, several water molecules, and Asp 13. Hydantocidin 5′-phosphate, GDP, HPO_4^{2-}, and Mg^{2+} may represent a set of synergistic inhibitors even more effective than the combination of IMP, GDP, NO_3^-, and Mg^{2+}.

The first committed step in the *de novo* biosynthesis of AMP is the formation of adenylosuccinate from GTP, IMP, and aspartate:

$$\text{GTP} + \text{IMP} + \text{L-aspartate} \rightleftharpoons \text{GDP} + P_i + \text{adenylosuccinate}$$

Adenylosuccinate synthetase [IMP: L-aspartate ligase (GDP-forming), EC 6.3.4.4] from *Escherichia coli* is a Mg^{2+}-dependent enzyme that catalyzes the above reaction by a two-step process (Lieberman, 1956; Fromm, 1958; Stayton *et al*., 1983; Webb *et al*., 1984; Bass *et al*., 1984; Cooper *et al*., 1986): (i) the transfer of the γ-phosphate of GTP to the 6-oxygen of IMP to form a 6-phosphoryl intermediate and (ii) the nucleophilic displacement of the 6-phosphate group by aspartate to form adenylosuccinate. Other mechanisms have been proposed for the action of (Miller & Buchanan, 1962; Markham & Reed, 1978), but all have the common feature of combining Mg^{2+}, aspartate, IMP, and GTP into a single active site.

In the absence of ligands, the active site of adenylosuccinate synthetase is disordered (Poland *et al*., 1993; Silva *et al*., 1995). Furthermore, the enzyme does not recognize the phosphate groups of GTP analogs in the absence of other substrates and Mg^{2+} (Poland *et al*., 1996). Crystal structures of the synthetase complexed with IMP, GDP, NO_3^-, Mg^{2+}, and hadacidin, however, clearly identify the ligand binding sites and conformational changes in the enzyme upon ligation (Poland *et al.*, 1997). The IMP complex implicates the β,γ-bridging oxygen in the binding of Mg^{2+}, providing a basis for the lack of recognition of β,γ-methylene-GTP by the synthetase even in the presence of Mg^{2+}.

Hydantocidin is a phytotoxin isolated from cultures of *Streptomyces hydroscopicus* (Nakajima *et al.*, 1991). It has potent herbicidal activity but low toxicity toward mammals (Nakajima *et al*., 1991). As a consequence, considerable effort is now focused on understanding the mechanism by which hydantocidin becomes selectively toxic toward plants. Apparently, hydantocidin is a proherbicide which requires phosphorylation of its 5′-OH for it to become active (Heim *et al*., 1995; Siehl *et al*., 1996). Hydantocidin 5′-phosphate (Figure 1) binds competitively with IMP to adenylosuccinate synthetase, exhibiting a K_i of 22 nM (Siehl *et al*., 1996; E. W. Walters, Sandoz Agro, Inc., unpublished).

Reported here is the crystal structure of the complex of adenylosuccinate synthetase from *E. coli* with hydantocidin 5′-phosphate, GDP, HPO_4^{2-}, Mg^{2+}, and hadacidin at 100 K (hereafter, the hydantocidin 5′-phosphate complex). Hadacidin (Figure 1), a fermentation product of *Penicillium frequentans* (Kackza *et al*., 1962), is a competitive inhibitor ($K_i \sim 10^{-6}$ M) with respect to aspartate (Clark & Rudolph, 1976; Markham & Reed, 1977). The synthetase here has nearly the same conformation as the enzyme ligated with IMP, GDP, NO_3^-, Mg^{2+}, and hadacidin (hereafter, the IMP complex; Poland *et al*., 1997). Hydantocidin 5′-phosphate

[†] This work was supported by Grants MCB-9316244 and MCB-9218763 from the National Science Foundation and by a gift from Sandoz Agro, Inc. This is Journal Paper No. J-16996 of the Iowa Agriculture and Home Economics Experiment Station, Ames, IA; Project No. 3159.

[‡] Coordinates for the structure described in this paper have been deposited with the Brookhaven Protein Data Bank (accession reference 1JUY).

* Corresponding author. Telephone: (515) 294-7103. Fax: (515) 294-0453. E-mail: honzatko@iastate.edu.

[§] Iowa State University.

[||] Sandoz Agro, Inc.

[⊗] Abstract published in *Advance ACS Abstracts,* November 15, 1996.

S0006-2960(96)01758-8 CCC: $12.00

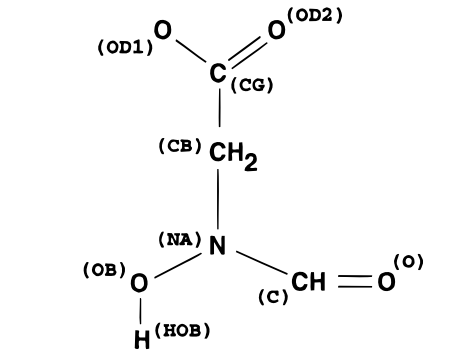

Hadacidin

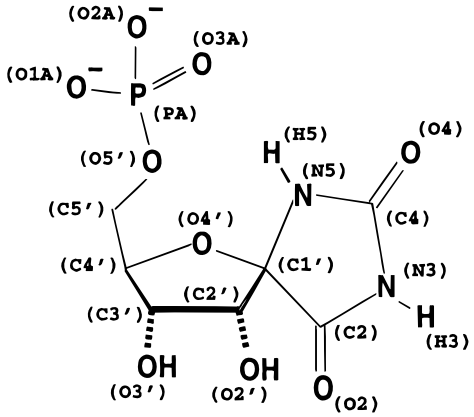

Hydantocidin 5′–phosphate

FIGURE 1: Diagram of hydantocidin 5′-phosphate and hadacidin, showing covalent linkages and names of atoms (in parentheses).

binds to the IMP region and the HPO_4^{2-} molecule to the NO_3^- region of the active site. The hydantocidin 5′-phosphate complex reveals an ordered active site, with each ligand clearly defined by the electron density.

MATERIALS AND METHODS

Adenylosuccinate synthetase was prepared as described previously from a genetically engineered strain of *E. coli* (Bass *et al*., 1987; Silva *et al*., 1995). The protein migrates as a single band on SDS−polyacrylamide gel electrophoresis with an apparent relative molecular weight of 48 000. Hydantocidin 5′-phosphate was synthesized by a procedure (to be published elsewhere) adapted from Mio *et al*. (1991). Hadacidin was a generous gift of Dr. Fred Rudolph and Dr. Bruce Cooper, Department of Biochemistry and Cell Biology, Rice University. All other reagents came from Sigma.

In the preparation of the hydantocidin complex, a fresh sample of pure hydantocidin 5′-phosphate was used. A stoichiometric amount of the hydantocidin inhibitor was added to the enzyme in order to avoid artifacts due to minor impurites that could arise during the period of crystallization and data collection. Crystals were grown by the method of hanging drops under conditions similar to those employed by Poland *et al*. (1997). In growing crystals of the hydantocidin 5′-phosphate complex, droplets contained 2 μL of enzyme solution [imidazole (50 mM), succinate (75 mM), GDP (4 mM), phosphate (4 mM), hydantocidin 5′-phosphate (0.4 mM), and protein (20 mg/mL) at pH 6.5] and 2 μL of a crystallization buffer [polyethylene glycol 8000 (13% w/w), cacodylic acid/cacodylate (pH 5.2, 100 mM), and magnesium acetate (200 mM)]. The final pH of the crystallization buffer was 6.5. Wells contained 500 μL of the crystallization buffer. Crystals of approximately 0.5 mm in all dimensions and belonging to the space group $P3_221$ ($a = b = 80.82$ and $c = 159.03$ at 100 K) grew in about 1 week. The asymmetric unit consists of a monomer of the synthetase dimer.

Table 1: Refinement Statistics for the Hydantocidin 5′-Phosphate Complex

resolution limit (Å)	2.6
number of measurements	181667
number of unique reflections	22503
completeness of data set (%)	99
completeness of data in the last resolution shell (%)	93 (2.7−2.6 Å)
R_{sym}[a]	9.4
number of reflections in refinement[b]	15536
number of atoms[c]	4850
number of solvent sites	233
R_{factor}[d]	0.195
R_{free}[e]	0.250
resolution (Å)	5−2.6
mean B (Å^2) for protein	22
rms deviations	
bond lenghts (Å)	0.012
bond angles (deg)	1.86
dihedral angles (deg)	24.9
improper dihedral angles (deg)	1.42

[a] $R_{sym} = \sum_j\sum_i|I_{ij}-\langle I_j\rangle|/\sum_i\sum_j I_{ij}$, where i runs over multiple observations of the same intensity and j runs over all crystallographically unique intensities. [b] All data in the resolution range indicated. [c] Includes hydrogens linked to polar atoms. [d] $R_{factor} = \sum||F_{obs}|-|F_{calc}||/\sum|F_{obs}|$; $|F_{obs}| > 0$. Based on all data from the final cycle of refinement. [e] R_{free} based upon 10% of the data randomly culled and not used in the refinement. Value taken from the penultimate round of refinement.

Data from a single crystal were collected on a Siemens area detector at Iowa State University and were reduced by using XENGEN (Howard *et al*., 1985). The data set was 99% complete to 2.6 Å resolution (Table 1).

Starting phases were calculated from the IMP complex (Poland *et al*., 1997), omitting IMP, NO_3^-, and hadacidin, as well as the solvent structure. Refinement of the structure involved manual fitting of models to the electron density, using a Silicon Graphics 4D-25 workstation and the program TOM (Cambillau & Horales, 1987), followed by a cycle of refinement using XPLOR (Brünger, 1992) on a Silicon Graphics 4D-35 workstation. Constants of force and geometry for the protein came from Engh and Huber (1991). The constants of force and geometry for hadacidin were taken from Poland *et al*. (1997). The phosphate molecule was refined as HPO_4^{2-}, that being the most likely substituent in the active site of the synthetase at pH 6.5. One oxygen of HPO_4^{2-} was in an environment consistent with the presence of an attached proton. As described below, however, several tautomeric forms of hydantocidin 5′-phosphate are possible, which could influence the site of protonation or even the state of protonation of the phosphate. Only one tautomer of hydantocidin 5′-phosphate, the 2- and 4-keto form (Figure 1), was considered in the refinement. In early rounds of refinement, the model was heated to 2000 K and then cooled in steps of 25 K to 300 K. In later rounds of refinement, the system was heated to 1000 or 1500 K but then cooled in steps of 10 K. After the slow-cooling protocol was completed (at 300 K), models were subjected to 120 steps of conjugate gradient minimization, followed by 20 steps of individual B parameter refinement. Individual B parameters were subject to the following restraints: nearest neighbor, main chain atoms, 1.5 Å^2; next-to-nearest neighbor, main

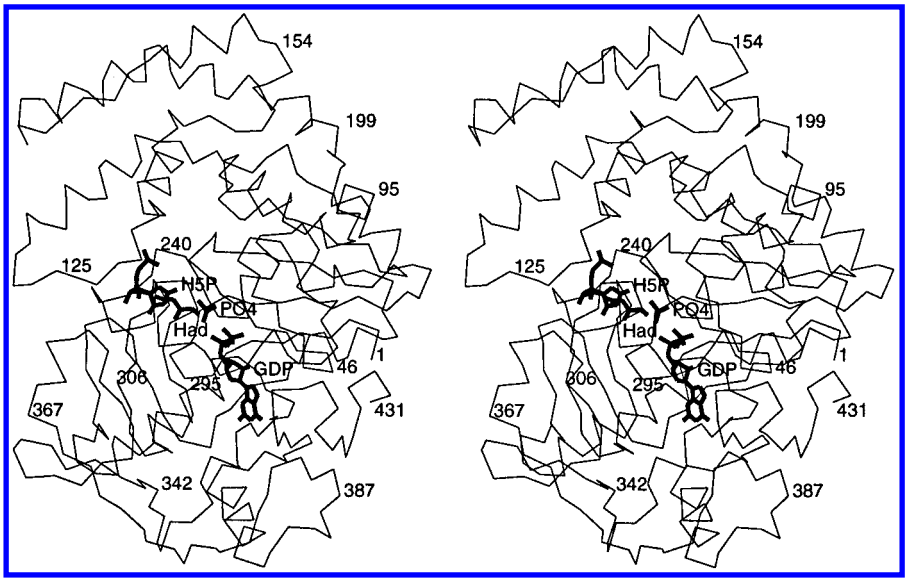

FIGURE 2: Stereoview of bound ligands in relation to a trace of α-carbons of adenylosuccinate synthetase.

chain atoms, 2.0 Å^2; nearest neighbor, side chain atoms, 2.0 Å^2; and next-to-nearest neighbor, side chain atoms, 2.5 Å^2.

Water molecules were added if (i) electron density at a level of 2.5σ was present in maps based on Fourier coefficients $(|F_{obs}| - |F_{calc}|)e^{i\alpha_{calc}}$ and $(2|F_{obs}| - |F_{calc}|)e^{i\alpha_{calc}}$ and (ii) acceptable hydrogen bonds could be made to an existing atom of the model. If after refinement a water molecule was beyond 3.3 Å from its nearest neighbor, it was deleted from the model. In addition, water molecules were deleted if their thermal parameters exceeded 80 Å^2. Harmonic restraints (5 kcal/mol) were placed on the positions of oxygen atoms of water molecules, in order to allow new water molecules to relax by adjustments in orientation. Occupancies of water molecules were not refined, because of the high correlation between occupancy and thermal parameters for data of 2.6 Å nominal resolution. Thus, solvent sites with *B* values between 50 and 80 Å^2 probably represent water molecules with occupancy parameters below 1.0 and thermal parameters substantially lower than those reported from the refinement.

RESULTS AND DISCUSSION

Quality of the Refined Models. Models for ligated adenylosuccinate synthetase have been deposited in the Protein Data Bank, Brookhaven National Laboratory. The method of Luzzati (1952) indicates an uncertainty in coordinates of 0.30 Å. The amino acid sequence used in refinement is identical to that reported by Silva *et al*. (1995) and differs at position 416 (glycine instead of aspartate) from the amino acid sequence deduced from the nucleotide sequence (Wolfe & Smith, 1988). Results of the refinement are in Table 1. The nominal resolution [where $\langle I/\sigma(I)\rangle = 2$] of the data set for the hydantocidin 5′-phosphate complex is 2.6 Å. Figure 2 provides an overview of the synthetase and bound ligands. Important ligand interactions are in Figure 3.

The Ramachandran plots (Ramachandran *et al*., 1963) are comparable to that of the IMP complex (Poland *et al*., 1997). The major outlier, as identified by the program PROCHECK (Laskowski *et al*., 1993), is Gln 10, which has been discussed in the literature (Poland *et al*., 1993; Silva *et al*., 1995). PROCHECK indicates better stereochemistry for the models than is typical for a structure of 2.5 Å resolution.

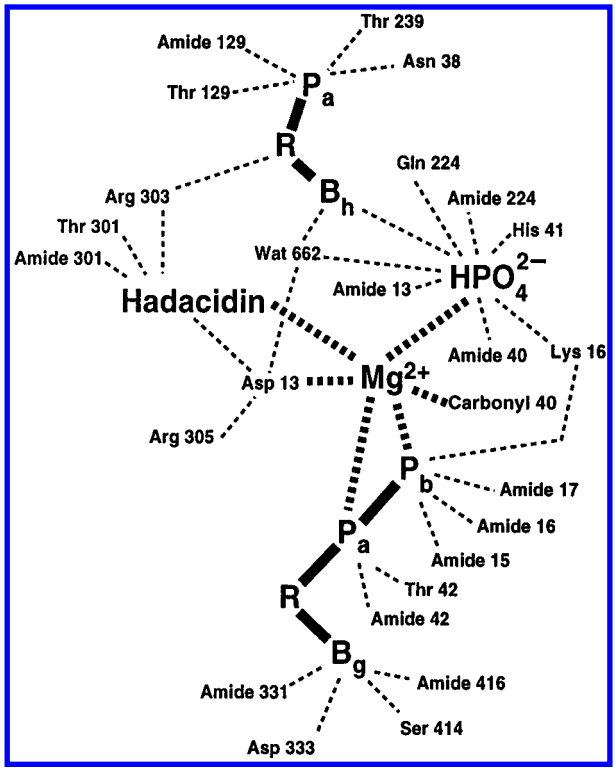

FIGURE 3: Diagram of hydrogen and coordinate bonding of the ligands: R, ribose; P_a, α-phosphate; P_b, β-phosphate; B_h, base of hydantocidin 5′-phosphate; and B_g, base of GDP.

Thermal parameters vary in the hydantocidin 5′-phosphate complex from 8 to 46 Å^2 for atoms of the main chain and from 6 to 52 Å^2 for atoms of side chains. The variation in the thermal parameter as a function of the residue number is similar to that reported by Poland *et al*. (1997) for the IMP complex.

Superposition of the hydantocidin 5′-phosphate and the IMP complex (Poland *et al*., 1997) gives a maximum deviation of 1.16 Å for α-carbons and 5.00 Å for side chains. The average root-mean-squared deviation in α-carbons is 0.27 Å. The root-mean-squared deviation in the coordinates of GDP, Mg^{2+}, and hadacidin (the ligands common to the IMP and hydantocidin 5′-phosphate complexes) is 0.56 Å, somewhat higher than the level of uncertainty in the coordinates. The large root-mean-squared difference in the

coordinates of GDP, Mg^{2+}, and hadacidin is due primarily to the relative displacement of the hadacidin molecules, presumably in response to the structural differences between IMP and hydantocidin 5′-phosphate.

Conformational changes between the hydantocidin complex and the unligated synthetase are similar to those reported for the IMP complex (Poland *et al*., 1997). Loop 42−53, which folds against the guanine nucleotide, exhibits an up to 9 Å movement. The conformational change is triggered by interactions between bound Mg^{2+} and backbone carbonyl 40 and between Thr 42 and the α-phosphate of GDP. The peptide linkage between residues 39 and 40 reorients, allowing carbonyl 40 to coordinate the Mg^{2+}. In addition, the peptide linkage between residues 223 and 224 also reorients so that backbone amide 224 can hydrogen bond to one of the oxygens of HPO_4^{2-} (see below). In unligated structures, both side chain and main chain atoms in the vicinity of residues 39 and 40 and 223 and 224 possess relatively high thermal parameters (Silva *et al*., 1995). Conceivably, even in the absence of ligands, these peptide linkages exist in more than one conformation. Another significant change involves a rotation of approximately 120° about χ^1 of His 41, causing the rupture of the salt link between His 41 and Asp 21 of the unligated structure and the formation of a new hydrogen bond between His 41 and HPO_4^{2-}. In addition to the above, loop 120−130 (described with respect to hydantocidin 5′-phosphate interactions) and loop 299−303 (described with respect to the binding of aspartate analogs) are well-ordered. The 10-stranded β-sheet that forms the central core of the monomer (Poland *et al*., 1993; Silva *et al*., 1995) undergoes little conformational change. Other modest conformational changes involve structural elements which connect the strands of this central β-sheet. As observed by Poland *et al*. (1997), these structural elements collapse toward the active site crevice.

GDP Binding Site. GDP in the hydantocidin complex exhibits interactions similar (Table 2, Figure 3) to those reported by Poland *et al*. (1997) in the IMP complex. Atom O6 of GDP interacts with OG of Ser 414 and backbone amide 331. Endocyclic N1 and exocyclic N2 of the base interact with the side chain of Asp 333. The 2′-OH of the ribose hydrogen bonds to a water molecule (Wat 582), which in turn hydrogen bonds to backbone carbonyls 42 and 417. In addition, the β-phosphate interacts with backbone amides 15−17, as well as with the Mg^{2+}. The α-phosphate of GDP interacts with the Mg^{2+} and the backbone amide and OG1 of Thr 42.

Differences in the interaction of GDP are observed, however, between the IMP and hydantocidin complex. In the IMP complex, ND1 of His 41 hydrogen bonds with the β-phosphate, while NE2 hydrogen bonds with a water molecule. In the hydantocidin 5′-phosphate complex, NE2 of His 41 hydrogen bonds with HPO_4^{2-} and ND1 hydrogen bonds with Glu 221. Lys 16, which binds exclusively with NO_3^- in the IMP complex, hydrogen bonds here with both HPO_4^{2-} and the β-phosphate of GDP. The subtle differences in the IMP and hydantocidin complexes demonstrate the "fluid" nature of the active site. A change in formal electrostatic charge from −1 (for NO_3^-) to −2 (for HPO_4^{2-}) may be responsible for the observed differences.

The guanine nucleotide in the hydantocidin 5′-phosphate complex is essentially identical in conformation to that reported by Poland *et al*. (1996, 1997). Torsion angles O5′−C5′−C4′−C3′ (γ by convention) and O4′−C1′−N9−C4 (χ by convention) have values of −67° (−*synclinal*) and −99° (*anti*), respectively. The pseudorotation phase angle of the ribose is 164° (2′-*endo*) [Saenger (1984) defines γ, χ, and the pseudorotation phase angle]. The pseudorotation phase angle differs from that of GDP in the IMP complex (3′-*exo*). The puckering of the ribose, however, cannot be determined unambiguously by X-ray data at a nominal resolution of 2.6 Å.

Hadacidin Binding Site. In the hydantocidin 5′-phosphate complex, hadacidin coordinates the Mg^{2+} through its *N*-formyl group and OB of hadacidin (Figure 1) hydrogen bonds to Asp 13 (Table 2 and Figure 4). The carboxylate of

Table 2: Selected Contacts Involving Ligands of the Hydantocidin 5′-Phosphate Complex[a]

ligand	ligand atom	contact atom	distanc (Å)
GDP	N2	OD2 of Asp 333	2.75
	N1	OD1 of Asp 333	2.91
	O6	OG of Ser 414	2.47
		N of Gly 416	3.06
		N of Lys 331	3.16
	N3	OW of Wat 645	2.69
	O2′	OW of Wat 582	2.62
	O3′	OW of Wat 713	2.79
		OW of Wat 712	3.21
	O1A	OW of Wat 553	2.79
		N of Thr 42	3.07
		OG1 of Thr 42	2.79
	O2A	Mg^{2+}	2.05
	O1B	N of Gly 17	2.99
		OW of Wat 553	2.45
	O2B	Mg^{2+}	1.92
	O3B	N of Gly 15	2.73
		N of Lys 16	2.61
		NZ of Lys 16	3.12
Mg^{2+}	Mg^{2+}	O2B of GDP	1.92
		O2A of GDP	2.05
		O3 of HPO_4^{2-}	2.26
		O of Gly 40	2.51
		OD1 of Asp 13	2.51
		O of hadacidin	2.00
HPO_4^{2-}	O1	NZ of Lys 16	3.15
		N of Gln 224	2.58
		NE2 of His 41	2.86
	O3	Mg^{2+}	2.26
		N of Gly 40	3.03
	O2	N of Asp 13	2.86
		NZ of Lys 16	2.78
		OW of Wat 662	2.70
	O4	NE2 of Gln 224	2.75
		O4 H5P[b]	2.92
hadacidin	O	Mg^{2+}	2.00
	OB	NH2 of Arg 305	2.51
		OD2 of Asp 13	2.51
	OD2	N of Thr 301	2.79
	OD1	NH2 of Arg 303	3.00
		OG1 of Thr 301	2.56
hydantocidin 5′-phosphate	O4	O4 of HPO_4^{2-}	2.92
	N3	OW of Wat 662	2.93
	O2	OW of Wat 555	2.74
	O2′	NH2 of Arg 303	2.80
		O of Val 273	2.93
		O of Gly 127	3.14
	O3′	OW of Wat 584	3.15
		OW of Wat 579	2.89
	O1A	N of Thr 129	2.66
		OG1 of Thr 129	2.44
		OW of Wat 583	2.67
	O2A	OW of Wat 609	2.88
	O3	ND2 of Asn 38	2.82
		OG1 of Thr 239	2.81
		OW of Wat 734	3.15

[a] Contacts listed are less than 3.4 Å. [b] Hydantocidin 5′-phosphate.

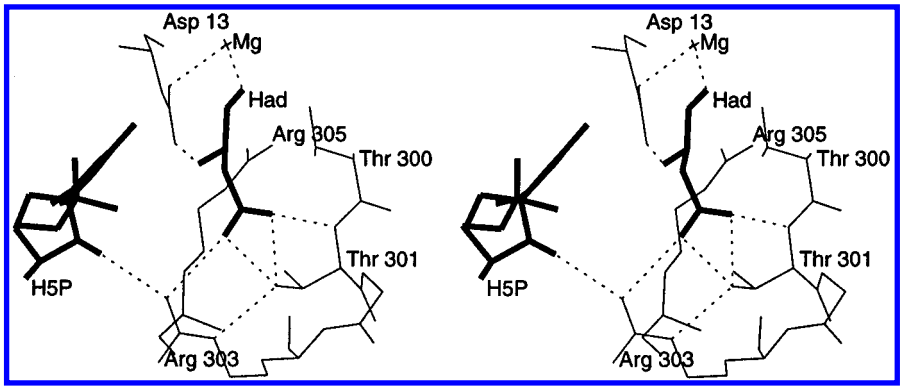

FIGURE 4: Stereoview of hadacidin in the active site. Dashed lines represent donor−acceptor interactions or coordinate bonds less than 3.2 Å long. Ligands are drawn with bold lines.

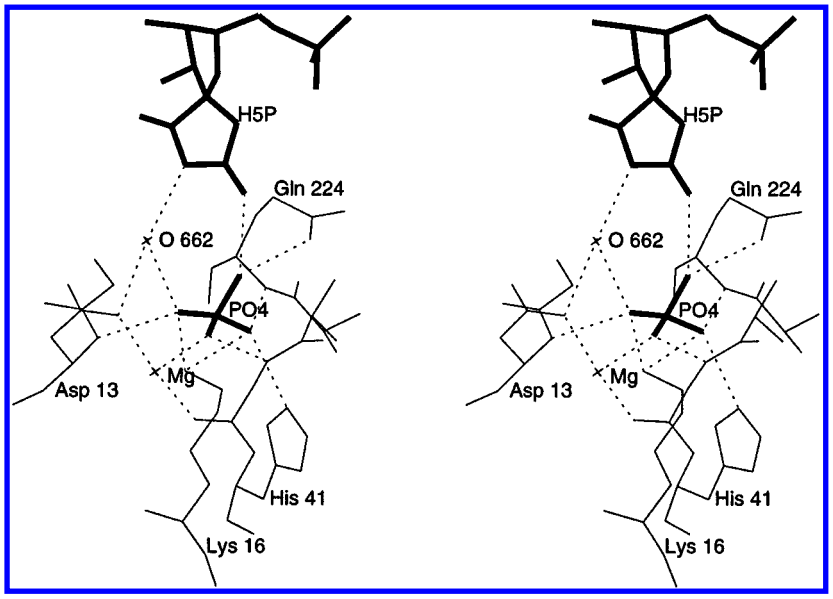

FIGURE 5: Stereoview of HPO_4^{2-} in the active site. Ligands are drawn with bold lines. Dashed lines represent donor−acceptor interactions or coordinate bonds less than 3.2 Å long.

hadacidin (structurally equivalent in the context of the active site to the β-carboxylate of aspartate) interacts with backbone amide 301 and OG1 of Thr 301. The interaction of the carboxylate of hadacidin mimics the putative stabilizing influence of negative electrostatic charge placed at the N-terminal side of α-helices (Richardson & Richardson, 1988). Residues 299−303 are disordered in all unligated and GTP-ligated structures of the synthetase (Poland *et al*., 1993, 1996; Silva *et al*., 1995). In the presence of hadacidin, however, loop 299−303 adopts an ordered structure similar to a single turn of α-helix. The dipoles of backbone amides 299−302 are oriented toward the carboxylate of hadacidin. These interactions are complemented by a salt link between that same carboxyl group and Arg 303. The interactions and conformation of hadacidin in the hydantocidin 5′-phosphate and IMP complexes (Poland *et al*., 1997) are the same within experimental uncertainty.

Mg^{2+} Binding Site. Six groups (backbone carbonyl 40, Asp 13, the α- and β-phosphates of GDP, HPO_4^{2-}, and hadacidin) position oxygen atoms within 2.6 Å of the Mg^{2+} (Table 2 and Figure 3). To within the uncertainty of the coordinates, Mg^{2+} exhibits octahedral symmetry in contrast to the IMP complex, where it exhibits square pyramidal coordination (Poland *et al*., 1997). The coordinate bonds which define the equatorial plane of the Mg^{2+} (the *N*-formyl oxygen of hadacidin and one oxygen each from HPO_4^{2-} and the α- and β-phosphates of GDP) average to 2.06 Å, as opposed to 2.30 Å for the corresponding bonds in the IMP complex. In the IMP complex, OD1 of Asp 13 hydrogen bonds with N1 of IMP and is 3.3 Å from the Mg^{2+}. In the hydantocidin 5′-phosphate complex, Wat 662 mediates the interaction between Asp 13 and hydantocidin 5′-phosphate. The Wat 662-mediated interaction may not fix the position of Asp 13 as effectvely as the direct IMP−Asp 13 interaction. As a consequence, the distance separating the Mg^{2+} and OD1 of Asp 13 decreases by approximately 0.8 Å and other coordinate bonds to Mg^{2+} relax to a new energy minimum structure. Changes in the position of Asp 13 relative to Mg^{2+}, in response to perturbations in its immediate environment, may modulate the pK_a of Asp 13 in a manner consistent with the proposed catalytic mechanism of the synthetase (Poland *et al*., 1997).

Phosphate Binding Site. HPO_4^{2-} occupies the same site as NO_3^- in the IMP complex (Poland *et al*., 1997). As a consequence, three of the four oxygen atoms of HPO_4^{2-} have interactions with the protein that are similar to those of NO_3^-. Oxygens of HPO_4^{2-} hydrogen bond with backbone amides 13, 40, and 224, as well as to the Mg^{2+} and the side chain of Lys 16 (Table 2, Figure 5). The interactions of HPO_4^{2-} differ from those of NO_3^- in several respects, however. His 41 hydrogen bonds with HPO_4^{2-} and not the β-phosphate of GDP, as observed in the IMP complex. In addition, the side chain of Gln 224 may form a bifurcated hydrogen bond to O4 of HPO_4^{2-} and to O4 of hydantocidin 5′-phosphate.

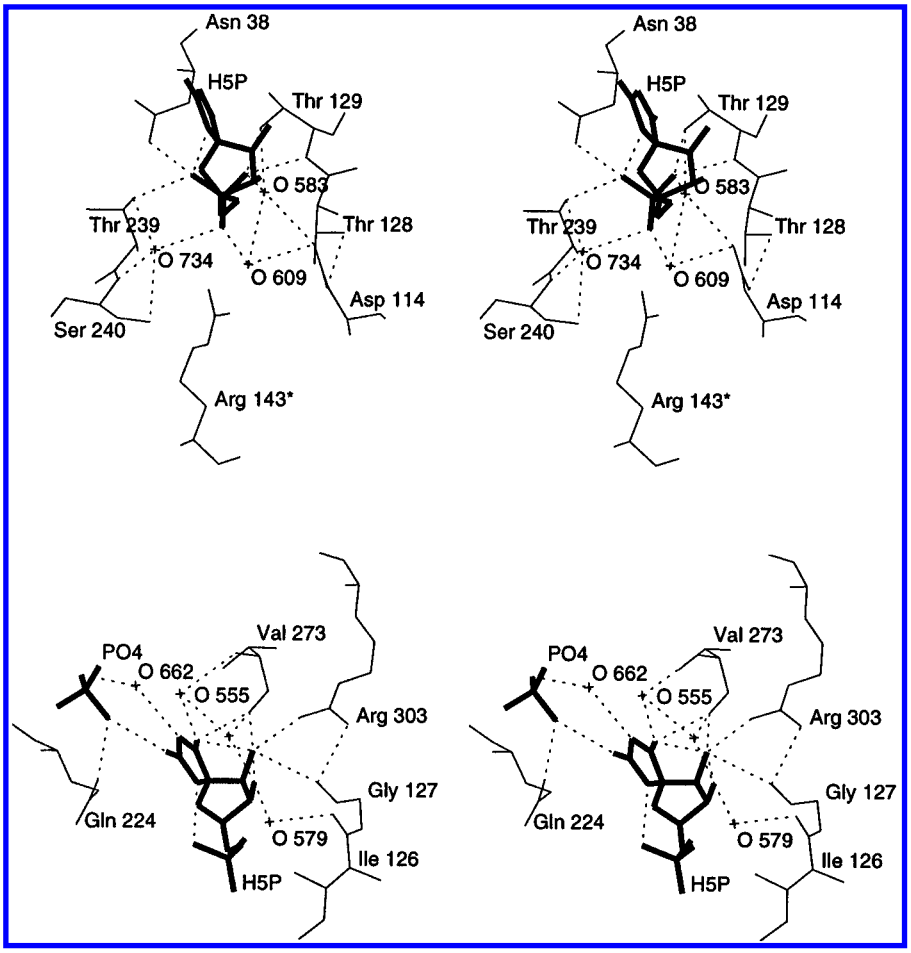

FIGURE 6: Stereoview of hydantocidin 5′-phosphate in the active site. Dashed lines represent donor−acceptor interactions or coordinate bonds less than 3.2 Å long. Ligands are drawn with bold lines: (top) interactions involving the α-phosphate and (bottom) interactions involving the ribose and base.

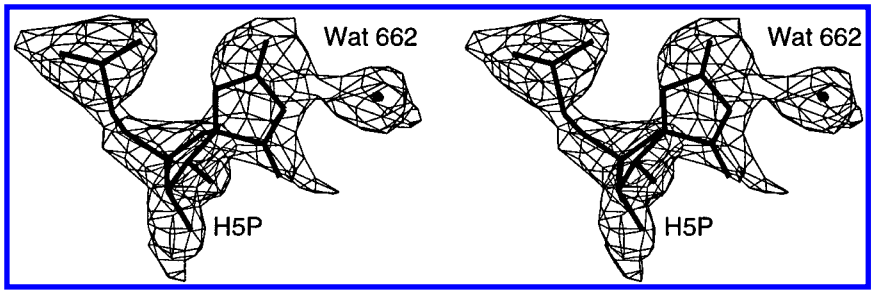

FIGURE 7: Stereoview of the electron density associated with hydantocidin 5′-phosphate and Wat 662 in the active site. The electron density is from a $2F_{obs} - F_{calc}$ map at a contour level of 6σ and a cover radius of 1.0 Å.

Finally O4 of HPO_4^{2-}, which bears the proton, hydrogen bonds as a donor to O4 of hydantocidin 5′-phosphate. The state of protonation of the phosphate, as well as the site of protonation, however, is subject to considerable uncertainty. For instance, hydantocidin 5′-phosphate may be in an alternative tautomeric state (4-enol rather than 4-keto), interacting with HPO_4^{2-} as a proton donor.

Hydantocidin 5′-Phosphate Binding Site. Recognition of hydantocidin 5′-phosphate by the synthetase is primarily through its 5′-phosphate. OG1 of Thr 129, backbone amide 129, ND2 of Asn 38, and OG1 of Thr 239 interact with the phosphate group of hydantocidin 5′-phosphate (Table 2, Figure 6). In addition, water molecules 583, 609, and 734 mediate interactions between the 5′-phosphate and the protein. Arg 143 from a symmetry-related monomer hydrogen bonds to the 5′-phosphate of IMP in the IMP complex but is nearly 3.5 Å from the 5′-phosphate of the hydantocidin inhibitor. The significance of Arg 143 has been demostrated by Leu 143 and Lys 143 mutants, each showing 100-fold elevations in the K_m for IMP, 10-fold elevations in the K_m for GTP, but no effect on the K_m for aspartate or k_{cat} (Wang *et al*., 1996).

The 2′-OH group of the ribose of hydantocidin 5′-phosphate hydrogen bonds to the guanidinium of Arg 303 and is in contact with four other oxygen atoms: (i) backbone carbonyl 127, (ii) backbone carbonyl 273, (iii) 3′-OH of the hydantocidin inhibitor, and (iv) 2-keto of the hydantocidin inhibitor (Figure 6, Table 2). The hydrogen atom associated with the 2′-OH falls in a potential energy well between backbone carbonyl 273 and the 3′-OH and 2-keto groups of hydantocidin 5′-phosphate. The contact between the 2′-OH and backbone carbonyl 127 (3.14 Å) is enforced by the interaction of each group with Arg 303. The 3′-OH hydrogen bonds with waters 579 and 555, which in turn interact with backbone carbonyls 126 and 273, respectively. Although the data are not of sufficient resolution to unambiguously

determine the state of puckering of the ribose of hydantocidin 5′-phosphate, the best fit to the electron density occurs with a low-energy 3′-*exo* conformation (pseudorotation phase angle, 206°). Torsion angle O5′−C5′−C4′−C3′ (γ by convention) is 45° (+*synclinal*).

Interactions between hydantocidin 5′-phosphate and OG1 of Thr 129, backbone amide 129, and backbone carbonyl 126 are apparently critical to the transformation of loop 120−130 from a state of disorder (Poland *et al*., 1993; Silva *et al*., 1995) into the well-defined conformation observed here. In addition to the interactions described above, Asp 114, Glu 118, and Arg 303 hydrogen bond to loop 120−130; these interactions are absent as well in the unligated synthetase. The binding of hydantocidin 5′-phosphate, as has been observed for IMP, stabilizes the conformation of at least one of two elements of poorly ordered structure of the unligated synthetase.

The base of hydantocidin 5′-phosphate interacts with Gln 224, HPO_4^{2-}, and waters 662 and 555 (Table 2, Figure 7). In fact, the base of hydantocidin 5′-phosphate participates in a network of hydrogen bonds involving Asp 13, Gln 224, HPO_4^{2-}, and the water molecules named above. Electron density associated with hydantocidin 5′-phosphate and Wat 662 appears in Figure 7.

Factors which may explain the high affinity of hydantocidin 5′-phosphate toward the active site of adenylosuccinate synthetase involve interactions within the inhibitor as well as interactions to other ligands and the enzyme. Hydantocidin 5′-phosphate as well as IMP bind to the active site with a γ (torsion angle O5′−C5′−C4′−C3′) of approximately 60°. In that conformation, the 5′-phosphate group approaches C8 of IMP and N5 of hydantocidin 5′-phosphate. In hydantocidin 5′-phosphate, a hydrogen bond bewteen N5 and the 5′-phosphate group stabilizes precisely that conformation preferred by the enzyme. In addition, hydantocidin 5′-phosphate lacks a conformational degree of freedom (the torsion angle χ) relative to IMP. Finally, the 2′-OH is probably an obligatory proton donor in an intramolecular hydrogen bond with the 2-keto group (Figure 1) of hydantocidin 5′-phosphate (donor−acceptor distance of 2.9 Å). The 2′-hydroxyl−2-keto interaction restricts the conformation of the ribose and requires that the 2′-hydroxyl be a proton acceptor in its hydrogen bond with the enzyme (note that the 2′-hydroxyl interacts with an obligatory proton donor, Arg 303). Apparently, a factor in the enhanced binding affinity of hydantocidin 5′-phosphate relative to IMP stems from a reduction in the entropic penalty associated with the selection of a specific conformer of IMP.

Hydantocidin 5′-phosphate, HPO_4^{2-}, GDP, and Mg^{2+} probably represent a synergistic combination of ligands, much like the combination of IMP, NO_3^-, GDP, and Mg^{2+} (Markham & Reed, 1977; Poland *et al*., 1997). The increased size of HPO_4^{2-} relative to NO_3^- is offset by a reduction in size of hydantocidin 5′-phosphate relative to IMP. Electrostatic interactions between NO_3^- and IMP (Poland *et al*., 1997) are replaced by hydrogen bonds between HPO_4^{2-} and the base moiety of hydantocidin 5′-phosphate. Synergistic binding is further indicated by kinetic studies in which hydantocidin 5′-phosphate interacts weakly with the synthetase unless aspartate, GTP (or GDP), HPO_4^{2-}, and Mg^{2+} are present (E. W. Walters, Sandoz Agro, Inc., unpublished results). With these ligands present, an apparent K_i of 22 nM was measured. Given the complexity of the active site, one would expect other ligand combinations to synergistically bind to the synthetase.

REFERENCES

Bass, M. B., Fromm, H. J., & Rudolph, F. B. (1984) *J. Biol. Chem. 259*, 12330−12333.

Bass, M. B., Fromm, H. J., & Stayton, M. M. (1987) *Arch. Biochem. Biophys. 256*, 335−342.

Brünger, A. T. (1992) *XPLOR: Version 3.1. A system for X-ray crystallography and NMR*, Yale University Press, New Haven and London.

Cambillau, C., & Horjales, E. (1987) *J. Mol. Graphics 5*, 174−177.

Clark, S. W., & Rudolph, F. B. (1976) *Biochim. Biophys. Acta 437*, 87−93.

Cooper, B. F., Fromm, H. J., & Rudolph, F. B. (1986) *Biochemistry 25*, 7323−7327.

Engh, R. A., & Huber, R. (1991) *Acta Crystallogr. A47*, 392−400.

Fromm, H. J. (1958) *Biochim. Biophys. Acta 29*, 255−262.

Heim, D. R., Cseke, C., Gerwick, B. C., Murdoch, M. G., & Green, S. B. (1995) *Pestic. Biochem. Physiol. 53*, 138−145.

Howard, A. J., Nielsen, C., & Xuong, N. H. (1985) *Methods Enzymol. 114*, 452−472.

Kaczka, E. A., Gitterman, C. O., Dulaney, E. L., & Folkers, K. (1962) *Biochemistry 1*, 340−343.

Laskowski, R. A., Mac Arthur, M. W., Moss, D. S., & Thornton, J. M. (1993) *J. Appl. Crystallogr. 26*, 283−291.

Lieberman, I. (1956) *J. Biol. Chem. 223*, 327−339.

Luzzati, V. (1952) *Acta Crystallogr. 5*, 802−810.

Markham, D. G., & Reed, G. H. (1977) *Arch. Biochem. Biophys. 184*, 24−35.

Markham, D. G., & Reed, G. H. (1978) *J. Biol. Chem. 253*, 6184−6187.

Miller, R. W., & Buchanan, J. M. (1962) *J. Biol. Chem. 237*, 485−490.

Mio, S., Kumagawa, Y., & Sugai, S. (1991) *Tetrahedron 47*, 2133−2144.

Nakajima, M., Itoi, K., Takamatsu, Y., Kinoshita, T., Okazaki, T., Kawakubo, K., Shindo, M., Honma, T., Tohjigamori, M., & Haneishi, T. (1991) *J. Antibiot. 44*, 293−300.

Poland, B. W., Silva, M. M., Serra, M. A., Cho, Y., Kim, K. H., Harris, E. M. S., & Honzatko, R. B. (1993) *J. Biol. Chem. 268*, 252334−25342.

Poland, B. W., Hou, Z., Bruns, C., Fromm, H. J., & Honzatko, R. B. (1996) *J. Biol. Chem. 271*, 15407−15413.

Poland, B. W., Fromm, H. J., & Honzatko, R. B. (1997) *J. Mol. Biol.* (in press).

Ramachandran, G. N., Ramakrishnan, C., & Sasisekharan, V. (1963) *J. Mol. Biol. 7*, 95−99.

Richardson, J. S., & Richardson, D. C. (1988) *Science 240*, 1648−1652.

Saenger, W. (1984) in *Principles of Nucleic Acid Structure*, pp 16−21, Springer-Verlag, New York.

Siehl, D. L., Subramanian, M. V., Walters, E. W., Lee, S.-F., Anderson, R. J., & Toschi, A. G. (1996) *Plant Physiol. 110*, 753−758.

Silva, M. M., Poland, B. W., Hoffman, C. R., Fromm, H. J., & Honzatko, R. B. (1995) *J. Mol. Biol. 254*, 431−446.

Stayton, M. M., Rudolph, F. B., & Fromm, H. J. (1983) *Curr. Top. Cell. Regul. 22*, 103−141.

Wang, W., Honzatko, R. B., & Fromm, H. J. (1996) *J. Biol. Chem.* (submitted for publication).

Webb, M. R., Cooper, B. F., Rudolph, F. B., & Reed, G. H. (1984) *J. Biol. Chem. 259*, 3044−3046.

Wolfe, S. A., & Smith, J. M. (1988) *J. Biol. Chem. 263*, 19147−19153.

BI961758R